Proc. Natl. Acad. Sci. USA
Vol. 92, pp. 758–762, January 1995
Neurobiology

Congenital myasthenic syndrome caused by prolonged acetylcholine receptor channel openings due to a mutation in the M2 domain of the ε subunit

KINJI OHNO*, DAVID O. HUTCHINSON*, MARGHERITA MILONE*, JOAN M. BRENGMAN*, CECILIA BOUZAT†, STEVEN M. SINE†, AND ANDREW G. ENGEL*‡

*Department of Neurology and Muscle Research Laboratory, and †Department of Physiology and Biophysics and Receptor Biology Laboratory, Mayo Clinic and Foundation, Rochester, MN 55905

Communicated by Clay Armstrong, University of Pennsylvania, Philadelphia, PA, October 21, 1994

ABSTRACT **In a congenital myasthenic syndrome with a severe endplate myopathy, patch-clamp studies revealed markedly prolonged acetylcholine receptor (AChR) channel openings. Molecular genetic analysis of AChR subunit genes demonstrated a heterozygous adenosine-to-cytosine transversion at nucleotide 790 in exon 8 of the ε-subunit gene, predicting substitution of proline for threonine at codon 264 and no other mutations in the entire coding sequences of genes encoding the α, β, δ, and ε subunits. Genetically engineered mutant AChR expressed in a human embryonic kidney fibroblast cell line also exhibited markedly prolonged openings in the presence of agonist and even opened in its absence. The Thr-264 → Pro mutation in the ε subunit involves a highly conserved residue in the M2 domain lining the channel pore and is likely to disrupt the putative M2 α-helix. Our findings indicate that a single mutation at a critical site can greatly alter AChR channel kinetics, leading to a congenital myasthenic syndrome. This observation raises the possibility that mutations involving subunits of other ligand-gated channels may also exist and be the basis of various other neurologic or psychiatric disorders.**

Congenital myasthenic syndromes (CMS) are inherited disorders in which the safety margin of neuromuscular transmission is compromised by one or more specific mechanisms. In contrast to myasthenia gravis, antibodies against the acetylcholine (ACh) receptor (AChR) are absent. Until now, the CMS have been characterized by clinical, morphological, and electrophysiological criteria. Those CMS identified to date include endplate (EP) acetylcholinesterase deficiency, presynaptic abnormalities that effect the release or size of transmitter quanta, or AChR deficiency with or without an associated kinetic abnormality of AChR (1). In the case of a kinetic abnormality detected at the single-channel level, a mutation involving an AChR subunit is likely. Identification of such mutations is of interest because they can provide insights into structure–function relationships of AChR and allow for genetic counseling and prevention. We report here discovery of a spontaneous mutation in human AChR. We show that the mutation leads to markedly prolonged openings of the AChR channel and is the cause of a CMS.

MATERIALS AND METHODS

Clinical Data. A woman, now 20 years old, had myasthenic symptoms since the neonatal period, a decremental electromyographic response on stimulation of motor nerves, negative tests for anti-AChR antibodies, and no history of similarly affected relatives. Previous studies of an intercostal muscle specimen from this patient at age 17 (2) revealed an EP myopathy with many degenerating junctional folds, abundant EP acetylcholinesterase, a reduced number (39%) of AChRs per EP, normal quantal release by nerve impulse, and reduced amplitude and a markedly prolonged and biexponential decay of miniature EP currents. Spectral analysis of AChR-induced current noise was best fitted by the sum of two lorentzians, consistent with two channel open times–one close to normal (1.9 ms) and one markedly prolonged (32.5 ms) (2). A second intercostal muscle specimen was obtained at age 18 for patch-clamp analysis of single AChR channel activity and for molecular genetic studies. Control muscle specimens were obtained from patients without muscle disease undergoing thoracic surgery. All human studies were in accord with the guidelines of the Institutional Review Board of the Mayo Clinic.

Patch-Clamp Studies of Endplate AChR. Small strips of intercostal muscle, intact from origin to insertion, were incubated at 37°C for 3–5 hr in oxygenated Tyrode solution (135 mM NaCl/5 mM KCl/2 mM $CaCl_2$/1 mM $MgCl_2$/15 mM $NaHCO_3$/1.3 mM Na_2HPO_4/11.1 mM dextrose, pH 7.2) containing 0.25 mg of collagenase (type I; Sigma) per ml. The strip was then transferred to collagenase-free Tyrode solution, and the nerve terminal and connective tissue were removed from EPs of individual fibers under Nomarski optics using fine microdissection (3). Patch pipettes were pulled from 7052 capillary tubes (Garner Glass, Claremont, CA), coated with Sylgard (Dow–Corning), and filled with dextrose-free Tyrode solution containing 1 μM ACh. AChR channel activity from the EPs was recorded from cell-attached and inside-out EP patches at 22°C. Recordings from more than one patch of an EP were combined for analysis. The initial pipette potential was 80 mV; when possible, recordings were also obtained at 40 and 120 mV. Single-channel currents were recorded using the Axopatch 200 amplifier (Axon Instruments, Foster City, CA), digitized at 50 kHz, stored on hard disk, and analyzed using PCLAMP 6 software (Axon Instruments). The effective bandwidth of the system was 5.2 kHz. Burst durations were determined by grouping openings separated by a specified critical time, t_c (4), which divided the briefest closed time component from the next longer component. Open interval and burst duration histograms were plotted by using a logarithmic abscissa and were fitted to the sum of exponentials by maximum likelihood (5).

mRNA and DNA Samples. mRNA was obtained from muscle with the Micro-FastTrack mRNA isolation kit (Invitrogen). First-strand cDNA was prepared from mRNA by using random hexamer primers with the cDNA Cycle kit

The publication costs of this article were defrayed in part by page charge payment. This article must therefore be hereby marked "*advertisement*" in accordance with 18 U.S.C. §1734 solely to indicate this fact.

Abbreviations: ACh, acetylcholine; AChR, ACh receptor; εT264P, Thr-264 → Pro mutation in AChR ε subunit; CMS, congenital myasthenic syndrome(s); EP, endplate; HEK, human embryonic kidney; SSCP, single-strand conformation polymorphism.

‡To whom reprint requests should be addressed.

(Invitrogen) and following the manufacturer's instructions. Genomic DNA was isolated from blood lysate or from proteinase/SDS digest of muscle by phenol–chloroform extraction followed by ethanol precipitation (6).

PCR Primers. Published cDNA sequences of the human α (7), β (8), δ (9), and ε (10) subunits were used to design cDNA primers. To amplify each exon and its adjacent splice donor and acceptor sequences from genomic DNA of each AChR subunit, we synthesized PCR primers according to intron sequences. For this, we used the known genomic sequence of the α subunit (7) but determined intron sequences of the β-, δ-, and ε-subunit genes first by using cDNA primers adjacent to putative introns predicted from genomic organizations in other mammals and then by sequencing the PCR-amplified intron regions. For the first exon of the β-, δ-, and ε-subunit genes, we used inverse PCR (11) to extend sequence information 5′ to the translational start sites and obtained 5′-end sequences for 142 bp of the β-, 196 bp of the δ-, and 562 bp of the ε-subunit genes (data not shown). This information enabled us to synthesize PCR primers to amplify each exon of the α-, β-, δ-, and ε-subunit genes.

PCR Procedures. PCR conditions for each primer were optimized by varying Mg^{2+} concentration and pH and by addition of 10% dimethyl sulfoxide for amplification of G+C-rich fragments. The typical PCR mixture included 60 mM Tris·HCl (pH 8.5), 15 mM $(NH_4)_2SO_4$, 1.5–2 mM $MgCl_2$, 0.10–0.25 mM each dNTP, 0.8 μM each primer, 100 ng of DNA, and 1.25 units of *Taq* DNA polymerase (Perkin–Elmer/Cetus) in 50 μl. cDNA fragments were amplified by the nested PCR procedure using 1/50th of the first amplification product. The typical cycling protocol comprised (*i*) denaturation at 94°C for 2 min; (*ii*) 35 cycles of 94°C for 30 sec, 55°C or 60°C for 30 sec, and 72°C for 3 min; and (*iii*) final extension at 72°C for 7 min.

We used allele-specific PCR to search for the demonstrated mutation in exon 8 of the ε-subunit gene in the patient's relatives and in normal control subjects. Primers were designed so that the 3′ end of the antisense primer was at the mutant site in ε gene exon 8. The antisense wild-type primer was 5′-ATG AGG AAC AAG AAG ACG GT-3′; the antisense mutant primer was 5′-ATG AGG AAC AAG AAG ACG GG-3′. The sense primer was 5′-CAA TGC CGA AGA GGT GGA GT-3′ in ε-subunit gene exon 6. The PCR procedure was optimized by adding 10% dimethyl sulfoxide and setting the annealing temperature to 60°C.

Single-Strand Conformation Polymorphism (SSCP) Analysis. The "cold" SSCP procedure was employed (12) with *ca.* 500 ng of PCR-amplified DNA. Denatured SSCP samples were loaded on a 4–20% gradient polyacrylamide gel, electrophoresed at 12°C, stained with ethidium bromide, and examined under ultraviolet light.

Sequence Analysis. PCR-amplified fragments of genomic DNA or cDNA were used for all sequencing procedures. PCR amplification products were purified by Wizard PCR Prep (Promega). cDNA fragments were used to sequence the entire open reading frame of the α- and β-subunit genes except for the first four nucleotides of the β-subunit gene, exon 8 of the ε-subunit gene, and exons 3 and 6–12 of the δ-subunit gene. Genomic DNA fragments were used to sequence the entire ε-subunit gene, exon 1 of the β-subunit gene, and the remaining exons of the δ-subunit gene. All fragments were sequenced with an Applied Biosystems model 373A DNA sequencer using fluorescently labeled dideoxy terminators. To confirm the mutation detected in exon 8 of ε-subunit DNA, we also sequenced this exon manually, using the *fmol* DNA sequencing system (Promega) and [α-^{33}P]dATP according to the manufacturer's recommendations and the antisense PCR primer as the sequencing primer.

Expression Studies. Mouse AChR α-, β-, γ-, and δ-subunit cDNAs were generously provided by John Merlie (Washington University, St. Louis) and Norman Davidson (California Institute of Technology); ε-subunit cDNA was a gift from Paul Gardner (13). cDNAs were subcloned into the cytomegalovirus-based expression vector pRBG4 as described (14). The εT264P mutation was constructed by bridging the *Nhe* I to *Bsp*MI sites in the ε-subunit cDNA with a synthetic double-stranded oligonucleotide harboring the Thr-264 → Pro mutation. The presence of the mutation and absence of unwanted mutations was confirmed by dideoxy sequencing of both the sense and antisense strands. Clonal 293 human embryonic kidney (HEK) fibroblasts were transfected with mutant or wild-type AChR subunit cDNAs by using calcium phosphate precipitation (14). The ratio of cDNAs used for transfection was 2:1:1:1 for α:β:δ:ε or εT264P, where 1 corresponds to 1.6 μg of cDNA per 35-mm-diameter plate of cells. Surface AChR expression by the 293 HEK cells was monitored by incubation with 10 nM ^{125}I-labeled α-bungarotoxin for 60 min at room temperature as described (14). Patch-clamp methods for studies of AChR expressed by 293 HEK cells were similar to those used at the EP except that cell-attached patches were used throughout, and the bath and pipette solutions were composed of 142 mM KCl, 5.4 mM NaCl, 1.8 mM $CaCl_2$, 1.7 mM $MgCl_2$, and 10 mM Hepes buffer (pH 7.4), with the pipette solution containing specified concentrations of ACh. Recordings were made with a membrane potential of −70 mV. The Gaussian filter was set at 5 kHz.

RESULTS AND DISCUSSION

Patch-Clamp Studies of EP AChR. Single-channel recordings from 7 EPs of the CMS patient were compared with those from 34 EPs of 8 control subjects. Simple inspection of the recordings from the CMS EP patches revealed a population of markedly prolonged channel openings (Fig. 1 *Left*). On formal analysis, both the open intervals and opening bursts at the control EPs had a very brief minor and a longer major component (Fig. 2 *Left Upper* and Table 1). At 6 CMS EPs, the open intervals and bursts had two components similar to those at the control EPs. In addition, a third, markedly prolonged component was present at patches of 4 CMS EPs (Fig. 2 *Left Lower* and Table 1). The above channel events at the CMS EPs, like >99% of the channel events at the control EPs, had a mean conductance of 60 pS. At the CMS EPs, we also observed an additional population of channel events, comprising 26% of the bursts, that had a reduced conductance of 46 pS. The open intervals and bursts of the 46-pS events had two components: a very brief one, whose duration was comparable to that of the very brief component of the 60-pS events at the control and CMS EPs, and a second more prolonged component (τ_2 = 5.1 ± 0.51 ms for the open intervals and 11.3 ± 0.79 ms for the bursts) (Fig. 2 *Right*). The conductance and time course of these channels suggested a persistent immature AChR containing the γ subunit in place of the ε subunit (15).

Two explanations for the patch-clamp data in the patient appeared likely, each postulating different species of AChR channels at the EP: (*i*) one wild-type channel and two mutant slow channels of differing conductance or (*ii*) one wild-type channel, one mutant slow channel of normal conductance, and a wild-type immature AChR.

Mutational Analysis. To investigate the possible genetic basis of the kinetic abnormality of AChR, we performed SSCP analysis on amplified fragments of the DNA encoding the ε and α subunits. Two aberrant conformers were detected. One was in a genomic fragment of the α subunit, was commonly found even in controls, and was shown to be due to a polymorphic insertion of a T nucleotide into intron 2, 5 bp upstream of the 5′ end of exon 3. The other was in exon 8 of the ε-subunit DNA and was unique to the patient. Sequencing of ε exon 8 using fragments of genomic DNA as well as cDNA disclosed a heterozygous A → C transversion at nucleotide

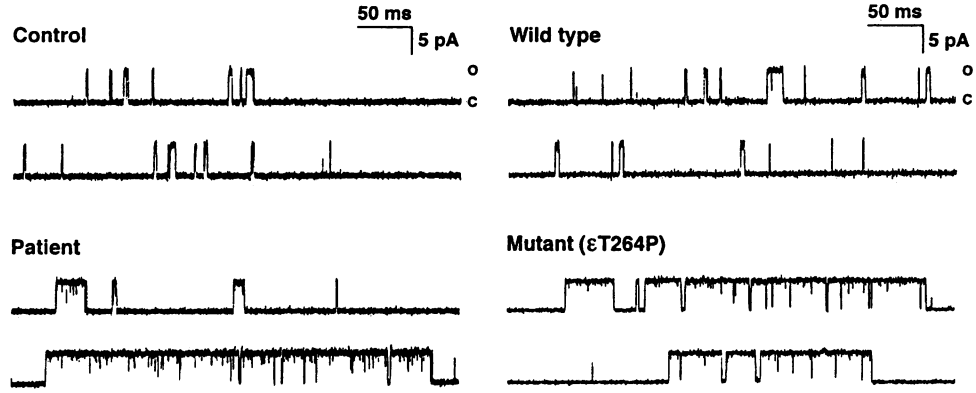

FIG. 1. Comparison of channel events recorded from normal human EP (*Left Upper*) and a CMS EP (*Left Lower*) and from HEK cells expressing wild-type (*Right Upper*) and mutant (*Right Lower*) AChR channels. Note occurrence of markedly prolonged channel events at CMS EP and in HEK cells expressing the εT264P mutation. ACh concentration = 1 μM.

790, converting the codon at position 264 encoding threonine to a codon encoding proline (Fig. 3 *Top*). The altered amino acid residue in the ε subunit is in the M2 membrane-spanning domain, which lines the pore of the AChR, and is the third residue C-terminal to the invariant leucine that may form the narrowest constriction of the channel (16).

Allele-specific PCR studies of the patient's family showed the heterozygous εT264P mutation only in the patient (Fig. 3 *Middle*), indicating its germ-line origin. The εT264P mutation was also not detected in DNA samples obtained from 100 controls and 9 other CMS patients. To ensure that there were no other mutations in the patient's AChR subunits, we sequenced the entire coding regions for the α, β, and δ subunits as well as the entire coding and noncoding regions for the ε subunit and found no other mutations. Multiple alignment of the AChR M2 segments showed that Thr-264 is conserved across the human α, β, and ε subunits and is highly conserved among the ε subunits of other species (Fig. 3 *Bottom*).

Expression Studies. To test whether the εT264P mutation alone leads to prolonged channel openings, we engineered the mutation into the ε-subunit cDNA of mouse AChR and coexpressed the mutant ε subunit with wild-type α, β, and δ subunits in HEK cells. Measurements of α-bungarotoxin binding revealed amounts of surface AChRs containing the mutant subunit ranging from 40% to 80% of AChRs containing the wild-type ε subunit. Patch-clamp recordings from the HEK cells expressing the mutant AChR revealed markedly prolonged channel open intervals and bursts (Fig. 1 *Right*) elicited by a range of acetylcholine concentrations (0.3–3 μM). Kinetic analysis confirmed the existence of prolonged channel events; in four patches, a major class of channels had a burst duration of 73 ± 7.5 ms (mean ± SEM). The corresponding kinetic parameter from the patient, 34.5 ms, though shorter, is in the same range as seen in the expression system. Quantitative differences in kinetics could arise from species differences (human versus mouse AChRs) or from different ionic compositions in the two sets of recordings. Analysis of channel amplitudes disclosed a single class of channels with a conductance of 68 pS, slightly lower than the 78 pS obtained for the wild-type adult mouse AChR, but clearly distinct from that of mouse AChRs containing the γ subunit (50 pS). The expression studies thus demonstrate close correspondence between channels produced by the εT264P mutation *in vitro* and the major class of anomalous channels observed at the patient's EPs (Fig. 1 *Right*).

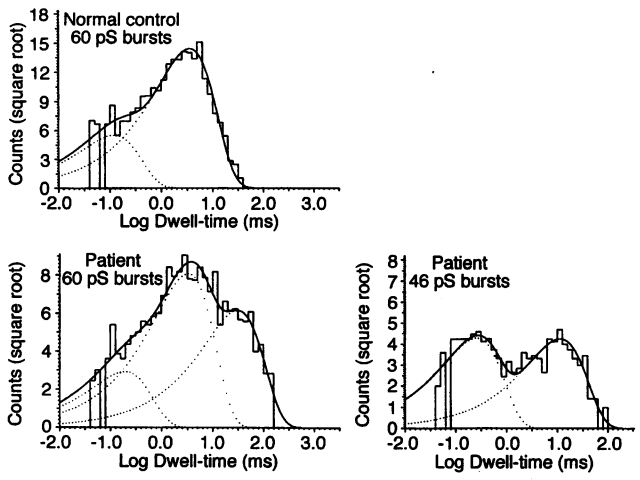

FIG. 2. Logarithmic histograms of the duration of AChR channel bursts at a control EP (*Left Upper*) and at a CMS EP (*Left Lower* and *Right*). The Gaussian filter was set at 7.5 kHz. Only 60-pS channels are active at the control EP. Both 60- and 46-pS channels are active at the CMS EP. Note the abnormally prolonged third component of the 60-pS bursts and the long second component of the 46-pS bursts at the CMS EP.

In addition to showing increased open interval and burst durations in the presence of ACh, the expressed mutant AChR exhibited an unusually high rate of spontaneous openings in the absence of ACh, ranging from 10 to 20 s^{-1} per patch, which is at least 2 orders of magnitude greater than that reported for native AChR (17). In ACh-free recordings, spontaneous bursts appeared as isolated events, contributing a single major component with a mean duration of 150 μs (Fig. 4 *Top*). In the presence of a range of ACh concentrations, spontaneous bursts contributed a component with the same mean duration but with an area that decreased with increasing ACh concentration (Fig. 4 *Middle* and *Bottom*). In parallel with the ACh-dependent decrease in spontaneous bursts, two classes of bursts with longer mean durations appeared that we associate with ACh occupancy (Fig. 4 *Middle* and *Bottom*). We hypothesize that these two classes correspond to openings by singly and doubly liganded AChRs because their areas show reciprocal changes over a 10-fold range of ACh concentration (18). Increased spontaneous and singly liganded bursts have also been reported for site-directed mutations in the α-subunit M2 domain (19).

Other Observations. The expression studies also suggested that the 46-pS channels detected at the patient's EPs were not mutant channels but were due to wild-type immature AChR containing the γ subunit (γAChR). Therefore, we searched for expression of γAChR at the patient's EPs in cryosections of muscle with an affinity-purified γ-subunit-specific antibody (20) (generously provided by Z. W. Hall, University of California at San Francisco) and a biotin-avidin-based detection system. The antibody, which recognized AChR in fetal but not in normal human adult muscle, revealed low levels of γAChR

Table 1. Open intervals and bursts of 60-pS channels at control and patient endplates

	Open intervals		Bursts	
Parameter	Controls	Patient	Controls	Patient
τ_1, ms	0.20 ± 0.022	0.20 ± 0.042	0.15 ± 0.019	0.25 ± 0.47
Area	0.16 ± 0.015	0.11 ± 0.016	0.16 ± 0.013	0.15 ± 0.027
EPs, no.	32	6	32	6
τ_2, ms	1.90 ± 0.085	2.54 ± 0.185	2.82 ± 0.16	3.96 ± 0.23
Area	0.85 ± 0.091	0.64 ± 0.090	0.85 ± 0.014	0.74 ± 0.043
EPs, no.	34	6	34	6
τ_3, ms	ND	10.2 ± 0.99	ND	34.5 ± 2.83
Area	ND	0.37 ± 0.093	ND	0.16 ± 0.063
EPs, no.		4*		4*

Values indicate means ± SEM. The area for each open-time component indicates the fraction of the dwell-time histogram area occupied by that component. ND, not detected.
*The third component of open intervals and bursts was present only at patches of four patient EPs.

at 6 of 13 EPs represented in the sections of the patient's muscle. We hypothesize that expression of the immature γAChR at the patient's EPs is a nonspecific compensatory reaction related to ongoing destruction and regeneration of the junctional folds. Indeed, we have now observed low levels of γAChR at the EP in cryosections obtained from two other CMS patients who had an associated EP myopathy but did not have the εT264P mutation.

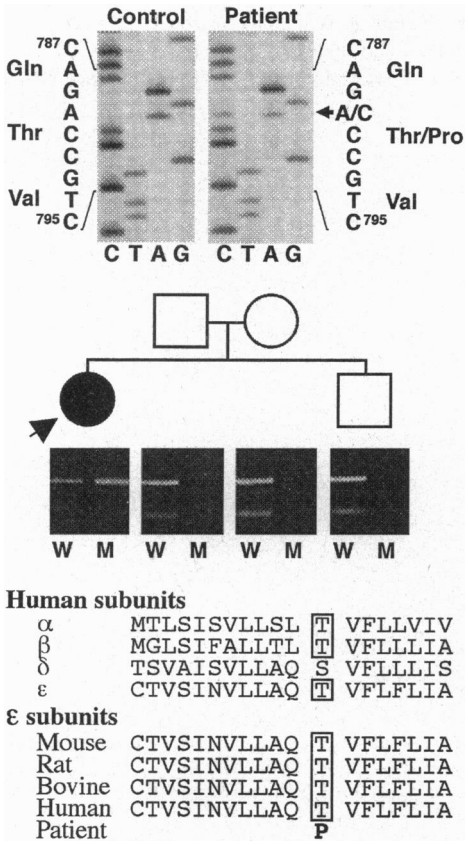

FIG. 3. (*Top*) Dideoxy sequencing of exon 8 of ε-subunit gene around codon 264 in DNA of CMS patient and a control. In patient, both A and C nucleotides are present at position 790 (arrow), indicating a heterozygous A → C transversion. This mutation changes codon 264 from an ACC codon for threonine to a CCC codon for proline. (*Middle*) Allele-specific PCR using genomic DNA from patient's muscle and from relatives' blood. Both the wild-type- and mutant-allele-specific primers amplified the expected 773-bp fragment (upper bands) in the patient, but only the wild-type primer amplified the expected fragment in the patient's parents and brother. Faint lower bands in relatives represent a PCR artifact. W, wild-type primer; M, mutant primer. (*Bottom*) Multiple alignment of AChR M2 segments. Boxes enclose the conserved threonine in other human AChR subunits and in AChR ε subunits of other species.

Pathogenicity and Significance of the εT264P Mutation. The εT264P mutation should be particularly pathogenic for the following reasons: (*i*) a single mutant allele produces disease; (*ii*) the mutation involves a residue highly conserved across species and subunits; (*iii*) the mutation occurs in the ε-subunit M2 domain, which contributes to the channel pore; and (*iv*) the substituted proline is conformationally restricted by its imino ring and can be expected to kink the putative α-helix of M2 (16), rendering it thermodynamically unstable (21, 22). This instability decreases free energy required for channel opening, as demonstrated by the increased rate of

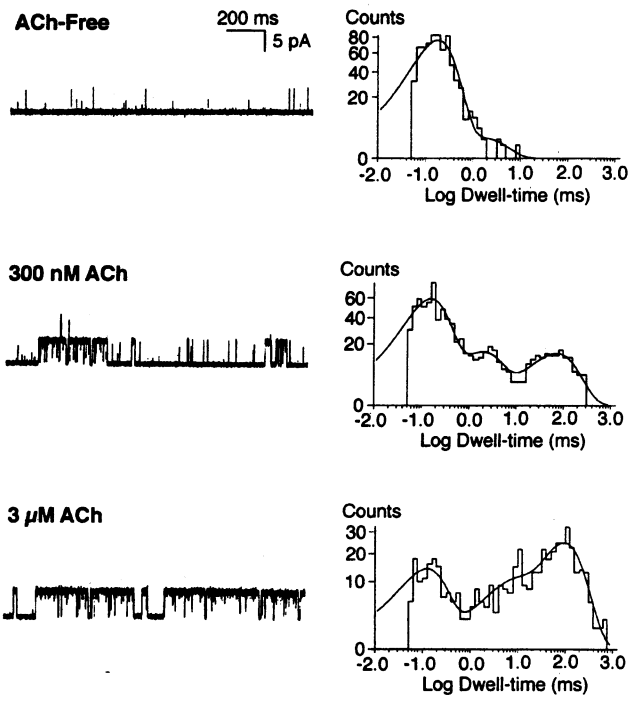

FIG. 4. Single-channel recordings of AChRs containing the εT264P mutant expressed in HEK cells. (*Left*) Single-channel currents elicited by the indicated concentrations of ACh. The membrane potential was −70 mV, and the Gaussian filter was set at 5 kHz. (*Right*) Burst-duration histograms corresponding to the traces on the left. The curves are sums of exponentials with the following fitted parameters for the ACh-free condition: τ_o = 174 μs, a_o = 0.97, τ_1 = 1.6 ms, and a_1 = 0.03; for the 300 nM ACh condition: τ_o = 150 μs, a_o = 0.67, τ_1 = 1.8 ms, a_1 = 0.16, τ_2 = 69.5 ms, and a_2 = 0.17; and for the 3 μM ACh condition: τ_o = 154 μs, a_o = 0.29, τ_1 = 5.8 ms, a_1 = 0.13, τ_2 = 93 ms, and a_2 = 0.58.

opening in the absence of ACh, and increases free energy required for channel closing, as demonstrated by the increased channel open duration. Increased openings of AChR in the absence of ACh could further enhance cationic overloading and destructive changes at the EP (1).

Our discovery of the εT264P mutation in the nicotinic AChR at the EP also implies that mutations involving subunits of neuronal AChRs and other central ligand-gated channels may also exist and be the basis of various neurologic and psychiatric disorders.

This work was supported by Grants NS6277 (to A.G.E) and NS31744 (to S.M.S) from the National Institutes of Health and by a research grant from the Muscular Dystrophy Association. Dr. Ohno is a Postdoctoral Fellow of the Muscular Dystrophy Association.

1. Engel, A. G. (1994) in *Myology*, eds. Engel, A. G. & Franzini-Armstrong, C. (McGraw–Hill, New York), 2nd Ed., Vol. 2, pp. 1798–1835.
2. Engel, A. G., Hutchinson, D. O., Nakano, S., Murphy, L., Griggs, R. C., Yu, G., Hall, Z. W. & Lindstrom, J. (1993) *Ann. N.Y. Acad. Sci.* **681,** 496–508.
3. Hamill, O. P., Marty, A., Neher, E., Sakmann, B. & Sigworth, F. J. (1981) *Pflügers Arch.* **391,** 85–100.
4. Sine, S. M., Claudio, T. & Sigworth, F. J. (1990) *J. Gen. Physiol.* **96,** 395–437.
5. Sigworth, F. J. & Sine, S. M. (1987) *Biophys. J.* **52,** 1047–1054.
6. Sambrook, J., Fritsch, E. F. & Maniatis, T. (1989) *Molecular Cloning: A Laboratory Manual* (Cold Spring Harbor Lab. Press, Plainview, NY), 2nd Ed.
7. Noda, M., Furutani, Y., Takahashi, H., Toyosato, M., Tanabe, T., Shimizu, S., Kikyotani, S., Kayano, T., Hirose, T., Inayama, S. & Numa, S. (1983) *Nature (London)* **305,** 818–823.
8. Beeson, D., Brydson, M. & Newsom-Davis, J. (1989) *Nucleic Acids Res.* **17,** 4391.
9. Luther, M. A., Schoepfer, R., Whiting, P., Casey, B., Blatt, Y., Montal, M. S., Montal, M. & Lindstrom, J. (1989) *J. Neurosci.* **9,** 1082–1096.
10. Beeson, D., Brydson, M., Betty, M., Jeremiah, S., Povey, S., Vincent, A. & Newsom-Davis, J. (1993) *Eur. J. Biochem.* **215,** 229–238.
11. Huang, S. H., Hu, Y. Y., Wu, C. H. & Holcenberg, J. (1990) *Nucleic Acids Res.* **18,** 1922.
12. Hongyo, T., Buzard, G. S., Calvert, R. J. & Weghorst, C. M. (1993) *Nucleic Acids Res.* **21,** 3637–3642.
13. Gardner, P. D. (1990) *Nucleic Acids Res.* **18,** 6714.
14. Sine, S. M. (1993) *Proc. Natl. Acad. Sci. USA* **90,** 9436–9440.
15. Mishina, M., Takai, T., Imoto, K., Noda, M., Takahashi, T., Numa, S., Methfessel, C. & Sakmann, B. (1986) *Nature (London)* **321,** 406–411.
16. Unwin, N. (1993) *J. Mol. Biol.* **229,** 1101–1124.
17. Jackson, M. B. (1986) *Biophys. J.* **49,** 663–672.
18. Colquhoun, D. & Sakmann, B. (1985) *J. Physiol. (London)* **369,** 501–557.
19. Sigurdson, W. & Auerbach, A. (1994) *Soc. Neurosci. Abstr.* **20,** 1132.
20. Gu, Y. & Hall, Z. W. (1988) *Neuron* **1,** 117–125.
21. von Heijne, G. (1991) *J. Mol. Biol.* **218,** 499–503.
22. O'Neil, K. T. & DeGrado, W. F. (1990) *Science* **250,** 646–651.